

Dynamic Characterization of a Seismic Isolated Viaduct Based on Vibration Measurements

F. Galvis, M. Bahamon, and E. E. Muñoz

Pontificia Universidad Javeriana, Bogotá-Colombia

J. P. Smith-Pardo

Seattle University, USA

J.A. Rodriguez

JEOprobe Ltda, Bogotá-Colombia



SUMMARY:

This manuscript presents a dynamic characterization of a curved 363-meter seismic isolated viaduct located in a moderate seismic hazard area near Bogotá-Colombia. The segmental structure consists of a post-tensioned hollow-core box girder supported on concrete piers with deep foundations. Seismic isolators are low-damping elastomeric bearings reinforced with steel plates. Tasks in the experimental/analytical program included measurement and processing of traffic-ambient vibrations, geophysical characterization of the soil, and development of site-specific ground motions. Linear time-history analyses and nonlinear static analyses of calibrated finite-element models of the soil-structure system are presented. It was found that simple structural models compare reasonably well with measured response. For the expected ground motions, it was also found that the seismic isolation system serves the purpose of limiting damage to the substructure despite of its negligible energy dissipation capability.

Keywords: base isolation, structural monitoring, ambient vibrations, seismic response

1. INTRODUCTION

In order to provide life safety and collapse prevention of engineered infrastructure, design engineers may proportion structures with the right balance between stiffness, strength and displacement capacity while preventing the occurrence of brittle modes of failure. Alternatively to this traditional approach and in order to minimize damage to non-structural elements, the use of external energy dissipation coupled with isolation devices (externally controlled or not) may be sought.

Seismic isolating devices may provide three basic features: i) vertical load bearing combined with flexibility under lateral loads such that the fundamental period of the isolated structure is increased and thus inertia effects are reduced, ii) energy dissipation so deformations of the isolating device may be maintained at tolerable levels, iii) appropriate lateral stiffness under operational loads. The design of seismically isolated bridge structures in the United States is customarily performed following the AASHTO Guide Specifications for Seismic Isolation Design (2010). For particular case of elastomeric bearings used as seismic isolation devices, AASHTO requires that the total shear strain (due to axial loads alone plus imposed seismic lateral displacements and rotation of the bearing) be less or equal than five.

2. DESCRIPTION OF THE STRUCTURE

Located at about 30km north of Bogotá, Portachuelo Viaduct (Fig. 1) is one the first applications of seismic isolation of bridges used in Colombia. The 363-meter segmental structure consists of a post-tensioned hollow-core box girder supported on concrete piers with deep foundations. The superstructure has 12 interior spans, each 27-meter long, and end spans of 20.2 and 19.2 meters length. The geometrical layout in plan consist of a spiral with radio of curvature of: i) 229m between one

abutment and the first interior support (support numbering is measured away from Bogotá), ii) 146m between the first and second support iii) 150m between the second and the ninth support, iv) 220m at supports 9th to 10th, v) 1018m between supports 10th and 11th, followed by a straight segment between supports 11th (through 13th) and the other abutment. The structure is also curved in elevation with the difference between abutments being 11.3m.



Figure 1. Portachuelo viaduct

The superstructure (Fig. 2a) consists of a post-tensioned hollow-core box with a total width of 10.3-meters (for two lanes, shoulders, and concrete barriers), which turns into a solid section at interior supports and abutments. The estimated superstructure weight is 130kN/m typically and changes to 180kN/m at supports and 310kN/m at the abutment. The superstructure support consists of two 1.4-meter concrete shafts supported by a 5.3x3x1.0-meter thick pile cap on six 0.6-meter diameter piles (Fig. 2b). Design 28-day compressive strength of concrete is 21MPa for piles and pile cap, 28MPa for shafts, and 35MPa for the superstructure. Reinforcement of shafts consists of 58-#8 longitudinal bars and #5 spirals at 75mm pitch within the first 2.3meters above the pile cap and at 150mm beyond the confinement zone.

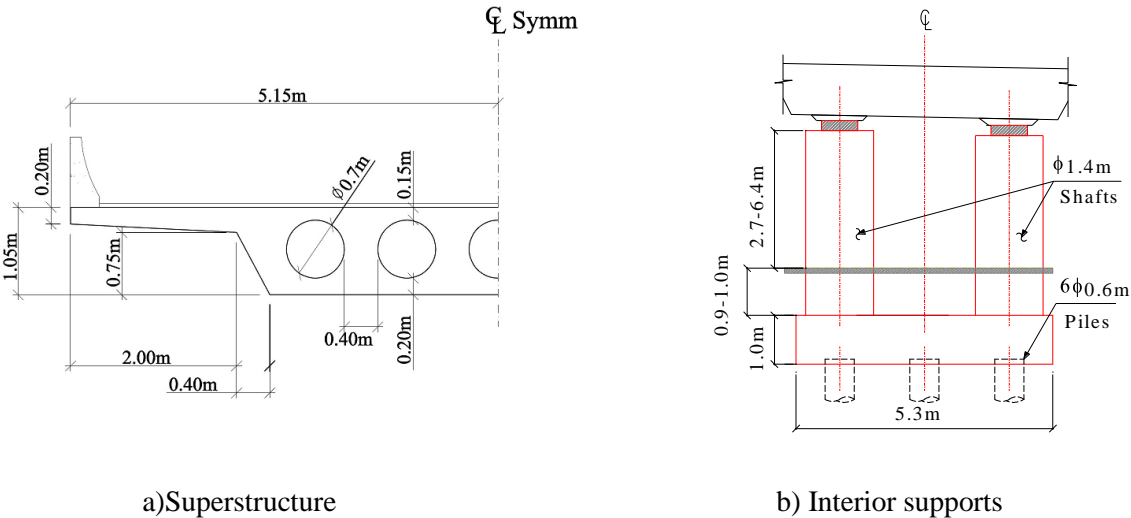


Figure 2. Structural configuration of Portachuelo Viaduct

Isolators consist of multi-layer low-damping rubber bearings (MLRB) bolted to the top of the shafts. Relevant geometrical properties are summarized in Table 2.1. In all cases, the thickness of each rubber layer is $t = 10\text{mm}$. Based on acceptance tests performed by the manufacturing company- AGOM International®, a shear modulus $G = 0.9\text{MPa}$ was selected to be representative for the isolators used in Portachuelo viaduct. This modulus is within the acceptance criteria under normal operation conditions established in the technical specification EN-1337-03:2005, which is $0.75 < G < 1.05\text{MPa}$.

Table 2.1. MLRB used in Portachuelo Viaduct

Support#*	Size (mm)	h(mm)	$\Sigma t(\text{mm})$
1-3, 10-13	$\phi 750$	210	155
4-6, 8, 9	$\phi 800$	250	185
7	$\phi 800$	270	200
Abutments	700x800	210	155

*refer to Fig. 5 for support numbering

Where, h: total isolator thickness, Σt : sum of rubber layer thickness, ϕ : diameter

3. SIMPLIFIED CALCULATIONS

Simple calculations are the most valuable tools to give confidence about the results obtained from elaborate (and, admittedly, obscure) finite elements models.

As at start, it is of value to evaluate and compare the lateral stiffness of the isolators and the supporting shafts. Consider for example support #6 (tallest pier). Assume that the isolator does not restrain the rotation at the top of the shaft –since it is expected to be sufficiently flexible- then:

$$K_{\text{shaft \#6}} = \frac{3EI}{L^3} = 12,200 \text{ to } 35,000 \text{ kN/m (cracked vs. uncracked section)} \quad (3.1)$$

where E is the modulus of elasticity of concrete, as calculated based on f'_c by using standard code provisions for bridge structures (AASHTO LRFD, 2010); $L = 7.4\text{m}$, is the distance from the bottom of the isolator to the top of the pile cap; and I is either the gross moment of inertia of the concrete section $I_g = \pi D^4/64$ or the cracked moment of Inertia, taken as $I_{cr} = 0.35I_g$ for simplicity.

The lateral stiffness of the isolator is given by:

$$K_{\text{isolator \#6}} = \frac{GA}{h} = 1,810 \text{ kN/m} \quad (3.2)$$

Where $G = 0.9\text{MPa}$, $h = 250\text{mm}$, and A is calculated based on the diameter of the isolator (Table 2.1).

The shaft stiffness is therefore between 7 and 20 times stiffer than the isolator, thus the assumption of a cantilever shaft element seems reasonable. The combined lateral stiffness of the system shaft-isolator (in series) at support #6 is between 1,720kN/m and 1,580kN/m which indicates that discussing whether one should use the gross moment of inertia versus the cracked moment of inertia for the shafts is unfruitful (as it is to distinguish between the two support shafts which differ in length by less than 5%).

The weight of the superstructure that is tributary to this shaft at support #6 is about $[180\text{kN/m} \times 5\text{m}$ (width of support) $+ 130 \text{ kN/m} \times (27\text{m}-5\text{m})]/2 = 1,880 \text{ kN}$, which is clearly more than the self weight of the shaft $24\text{kN/m}^3 \times (\pi \times 1.4^2)\text{m}^2/4 \times 7.4\text{m} = 270 \text{ kN}$. It is noted that the normalized axial stress on the shafts $P/(A_g f'_c) = (270+1880)/[(\pi \times 1.4^2)/4 \times 28,000] = 0.05$ (where A_g is the gross cross-sectional area of the shaft) is rather small so that under lateral loads one could expect a ductile response (tension

controlled) in flexure, provided that the shafts are not weaker in shear and the longitudinal reinforcement is properly anchored.

The fundamental period an equivalent single degree of freedom (SDOF) system can now be estimated as (using half of the mass of the shaft as tributary to the oscillation and the average of the lateral stiffness of the system calculated above)

$$T_{\text{sup port \#6}} = 2\pi \sqrt{\frac{(1,870 + 135) / 9.8}{(1,720 + 1580) / 2}} = 2.2 \text{ sec} \quad (3.3)$$

Following the same approximation, the fundamental periods of the individual supports of Portachuelo Viaduct –as SDOF- are calculated to be between 1.9 and 2.2seconds.

The moment capacity of any of the shafts in Portachuelo was calculated as $M_n = 7,700\text{kN-m}$ using conventional strain compatibility and for an axial compression of 2,000kN (average dead load per shaft). Then, the shear corresponding to flexural hinging of shaft#6 is given by:

$$V_y = 7,700\text{kN-m}/7.4\text{m} = 1,040\text{kN} \quad (3.4)$$

And the corresponding base shear coefficient is:

$$V_y/W = 1,040/(1880+270) = 0.48. \quad (3.5)$$

For the shortest shafts at support #1 ($L = 3.7\text{m}$), the shear coefficient is as high as 0.96.

This implies that give the high fundamental period of the SDOF system and also its high base shear capacity, yielding in flexure may be unlikely to occur given that the viaduct is not located in a high seismic risk region.

The calculated shear capacity of the shaft, conservatively ignoring axial compression, is approximately calculated using a re-arranged version of the AASHTO LRFD (2010) simplified equation for non-prestressed members:

$$V_{\text{shear}} = (v_c + \rho_v f_{yt}) 0.8D^2 = 3,900\text{kN} \quad (3.6)$$

Where, v_c is the unit shear strength of concrete $= 0.17 \sqrt{f'_c}$, where $f'_c = 28 \text{ MPa}$ is the design 28-day concrete compressive strength, ρ_v is the spiral reinforcement ratio for #5 bars at 150mm pitch, f_{yt} is the yielding stress of the spiral and effective shear depth, and D is the shaft diameter = 1.4 m.

Even, if one would argue that the contribution of concrete to shear capacity is negligible (because of the low axial compression due to dead load) $V_{\text{shear}} = 2,600\text{kN}$, thus it is apparent that the lateral load capacity of the Portachuelo Viaduct is not controlled by the shear but the flexural capacity of the shafts.

Assuming that the isolator remains elastic, the displacement of shaft-isolator #6 corresponding to the formation of a flexural hinge at the base of the shaft is given by (in this case, it is more appropriate to use the cracked moment of inertia of the shaft in the combined stiffness of the system isolator/shaft)

$$\Delta_y = 1,040\text{kN}/(1,580\text{kN/m}) = 0.66\text{m} \quad (3.7)$$

From which $0.66\text{m} \times 1,580/1,810 = 0.57\text{m}$ corresponds to shear deformation of the isolator (a rather high, but still tolerable, shear strain of $570/250 = 2.28$ as can be found in Stanton et al. 2008) and only 0.09m corresponds to drift of the shaft itself.

4. GROUND MOTIONS

A geophysical characterization of the soil was performed in order to develop site-specific ground motions. This included seismic geophysical tests using a digital seismograph and 24, 4.5Hz natural frequency, geophones at 5-meter spacing. Measurements were made of surface excitation created by dropping a 27-kg hammer on a steel plate, and ambient noise (mainly traffic) . Shear wave velocity (V_s) profiles were obtained by the method of dispersion of surface waves (ReMi) . One of the profiles varies from 200m/s at the surface to 400m/s at a depth of 50m, whereas the other profile varies from about 300m/s to 500m/s. Rock was estimated to be at 75-meter depth.

Because of the geographical proximity of the Portachuelo Viaduct to Bogotá, the same records used to develop the seismic zoning of the city were implemented (Martinez et al. 2002); these included a total of eleven near, intermediate and far source seismic records. The software DEEPSOIL was used to conduct 1D equivalent linear analysis of the site by incorporating stiffness and damping functions proposed by Vucetic and Dobry (1991). Figure 3 shows the envelope (of eleven records) of the site-specific acceleration spectra for the two developed shear wave velocity profiles and the Colombian seismic design of bridges code (Ministerio de Transporte 1995).

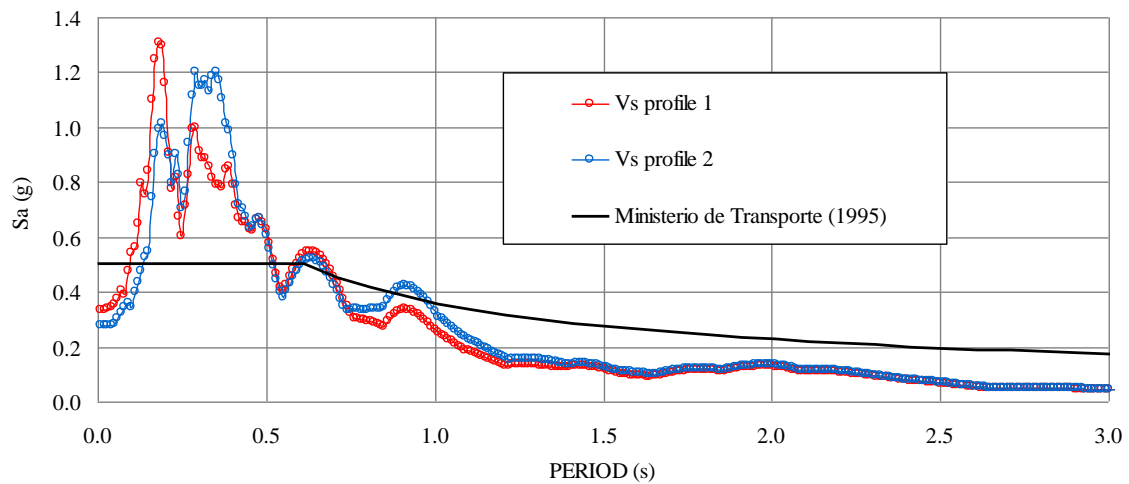


Figure 3. Site-specific acceleration spectra and Colombian code spectra

It is apparent that for the estimated fundamental period of the structure (around 2.0 sec) the elastic base shear coefficient is only 0.2, which is significantly less than the minimum base shear capacity coefficient calculated in the previous section ($V_y/W = 0.48$). Thus one would expect that under the selected ground motions, flexural hinging of the shafts would be unlikely to occur.

5. VIBRATION INSTRUMENTATION PROGRAM

Two alternative protocols were implemented in the instrumentation program that used 6 unidirectional accelerometers. In the first protocol acceleration responses in the longitudinal direction and transverse direction of the viaduct were consequently measured on a support-by-support basis; two accelerometers were placed on the ground near the shafts, two more at the top of the shafts (adjacent to the isolators) and two at the level of the surface of the superstructure. Collected data was decimated to 50 data points per second and subsequently filtered to frequencies between 0.3 and 10 Hz using a Butterworth filtering technique. The frequency response functions (FRF) at the top of the shafts and at the top of the superstructure were calculated relative to that at the level of the ground:

$$\text{FRF}(\omega) = \frac{\text{PSD}_{XY}}{\text{PSD}_{YY}} \quad (5.1)$$

where, PSD is the power spectral density function (calculated using crossed Fourier's transforms), X is the measured signal (top of the shaft and superstructure) and Y is the measured signal at the surface of the ground. Typical calculated FRF are shown in Fig. 4 for support #13 (adjacent to an abutment).

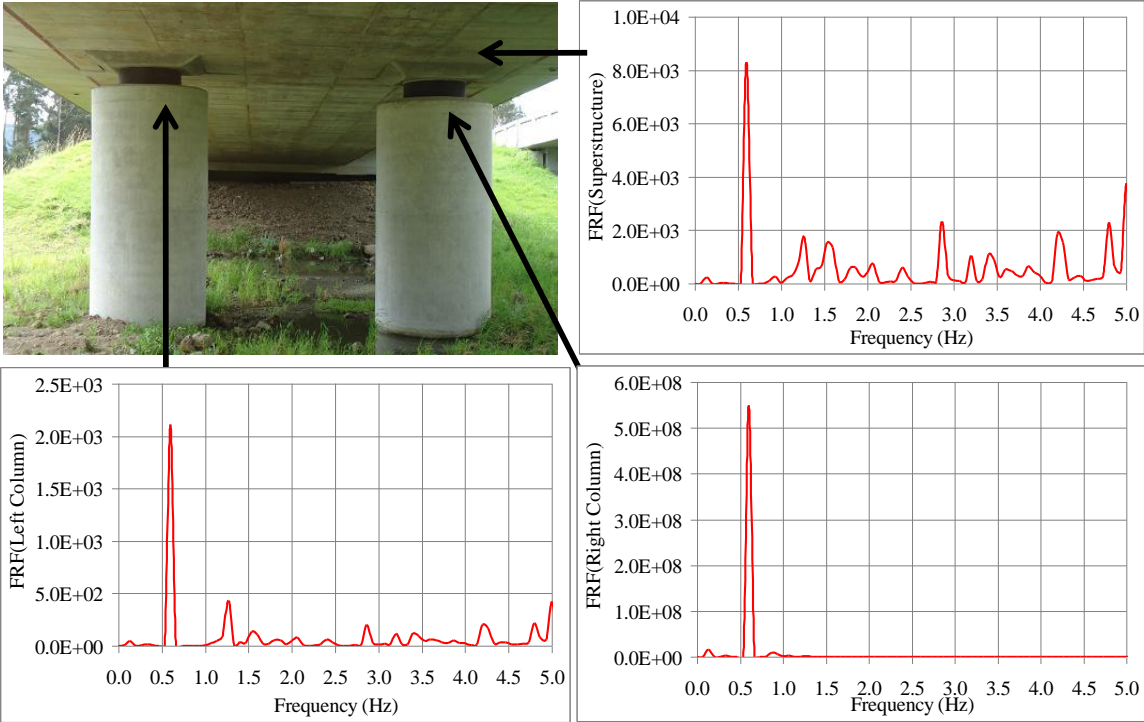


Figure 4. Frequency Response Functions at Support #13

In all 13 supports, a peak value in the response function was observed near the 0.5Hz frequency, which is consistent with the preliminary calculations as a SDOF for which an average fundamental period of 2.0 seconds was estimated. Table 4.1 presents a comparison of the calculated periods for the individual supports as SDOF with the measured period (=1/frequency) corresponding to the highest peak in the frequency response function (FRF). It is observed that despite of its simplicity, the SDOF approximation provides reasonable results.

Table 4.1. Measured and Calculated Periods at Supports of Portachuelo Viaduct

Support#	Calc. SDOF T(s)	Period at FRF Peak Value		Measured/Calc.	
		Long. (s)	Radial (s)	Long. (s)	Radial (s)
1	1.89	1.80	1.76	0.95	0.93
2	2.04	1.84	1.90	0.90	0.93
3	2.09	1.69	1.71	0.81	0.82
4	2.13	1.79	1.96	0.84	0.92
5	2.14	1.82	2.19	0.85	1.02
6	2.19	1.90	2.31	0.87	1.05
7	2.22	1.59	2.08	0.71	0.94
8	2.13	1.82	2.00	0.85	0.94
9	2.15	1.98	1.70	0.92	0.79
10	2.06	1.93	1.77	0.94	0.86
11	2.04	1.94	1.80	0.95	0.88
12	2.05	2.04	1.80	1.00	0.88
13	1.86	1.74	1.65	0.93	0.89

In the second instrumentation protocol, acceleration records were obtained at the level of the riding surface of the viaduct only and following recommendations given in the literature (Ventura et al. 2003). Due to the limited equipment, one of the accelerometers was kept fixed (as reference) and the remaining accelerometers were changed into two alternative setups as shown in Fig. 5.

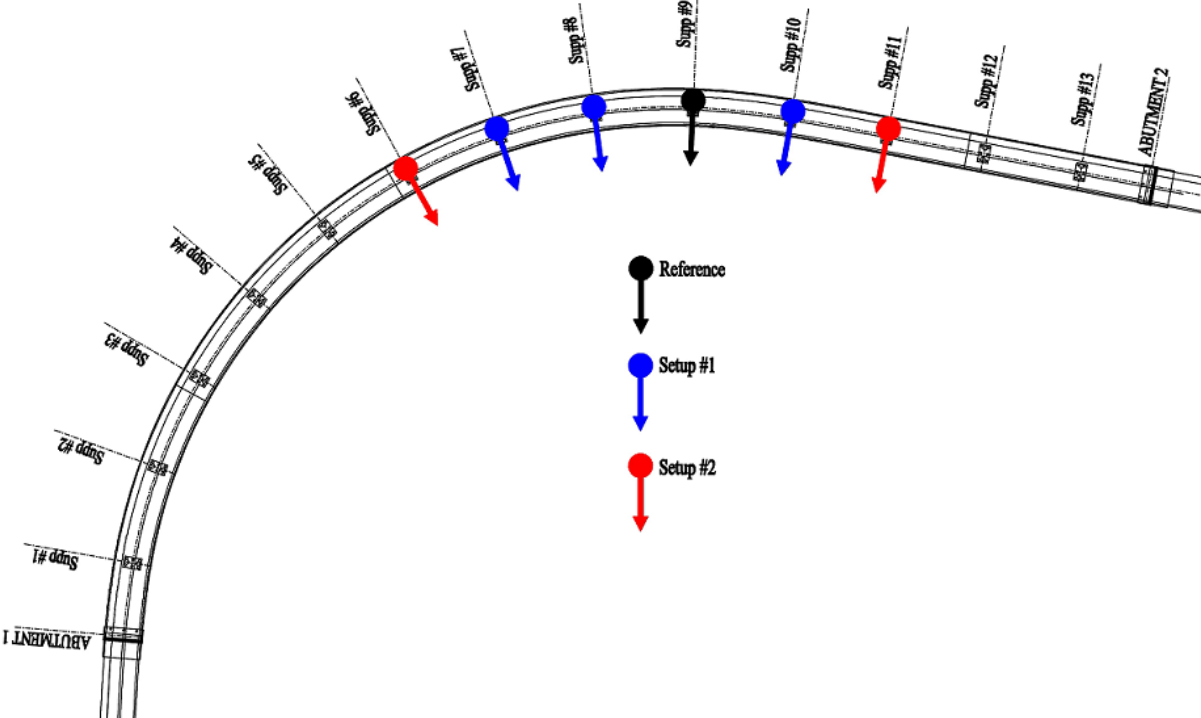


Figure 5. Acceleration Setups for Second Instrumentation Protocol

The accelerometers placed at supports# 6, 7, and 8 were used to measured vibrations in the global transverse direction, whereas accelerometers in supports #10 and 11 were used to measure vibrations in the global longitudinal direction. The global longitudinal direction was defined as a straight line that connects the two abutments at the ends of the viaduct, whereas the global transverse direction is perpendicular to the former.

For each station, a normalized power spectra density (NPSD) was calculated as the ratio of the power spectra at each frequency and the sum of all the PSD. An average normalized power spectra density (APSD) is further calculated using all the records in order to represent the entire structure.

Following this protocol, peak values for the NPSD were observed at frequencies of 0.51 Hz in the global longitudinal direction and 0.52 Hz in the transverse direction. These measured frequencies are consistent with the results obtained in the first protocol and also with the preliminary SDOF fundamental period calculation of the structure.

6. NUMERICAL MODELING

Linear elastic finite element models of the Portachuelo Viaduct were created in order to confirm the expected behaviour that was inferred from simple SDOF analyses and determine additional dynamic characteristics, and time-history force demands under ground excitation. The computer program SAP2000® was employed for this purpose. In one of the models, depicted in Fig. 6, the superstructure is modelled as frame element (spine) supported on shafts (also as modelled frames) that are fixed at their base. A variation of this consisted in modelling the deep foundation by means of a plate element

supported by piles that are laterally restrained by soil springs or py-curves (Matlock (1970), and Reese et al. (1974)). Alternative models considered the superstructure as plate elements and the substructure as frames (shafts) fixed at their bases or supported on a group of piles restrained laterally by soil springs (Fig. 7). 5% structural damping was considered in all cases and energy dissipation. Isolators were modelled as lineal elastic members with no energy dissipation capability.

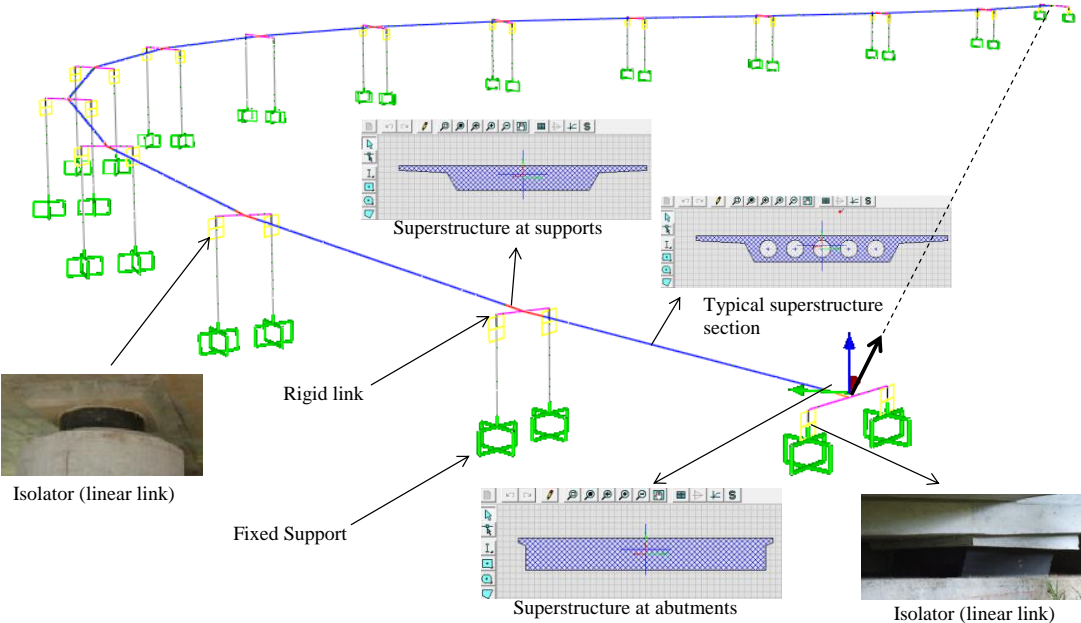


Figure 6. Spine model for superstructure and fixed base for shafts

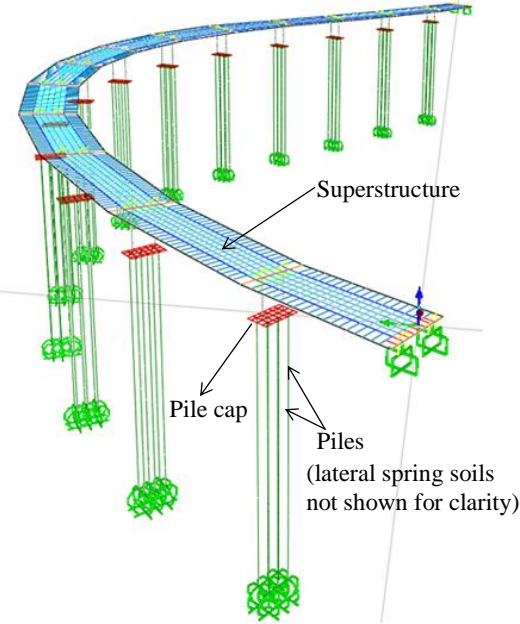


Figure 7. Plate model for superstructure and flexible base for shafts

As anticipated, modelling the superstructure as frame or as plate elements does not make a significant difference in the dynamic response (fundamental periods are within 5%) because, by virtue of the isolators, the superstructure mostly moves as a rigid body and thus the only aspect that matters is the mass distribution (which is modelled closely the same in both cases). Accounting for the flexibility of the supports obviously had the effect of elongating the period but only by 10% approximately (i.e., the structural model with piles and soil springs is about 20% more flexible than that of the fixed shafts).

Taking averages of the four models, the estimated period in the global longitudinal direction (defined as the line connecting the two abutments) was found to be 1.95sec, whereas the period in the global transverse direction (perpendicular to the longitudinal direction) was found to be 1.91sec. Given the level of uncertainty in some of the input variables, one could not warrant more than two significant figures in the calculation of the fundamental period and thus claim that it is essentially the same in the two orthogonal directions as hinted by the simplified SDOF analysis shown in Section 2 of this manuscript. Once again, it is apparent that the SDOF simplification proves to be quite reasonable since it renders periods around 2.0 seconds for the different supports.

A series of elastic time-history analyses were conducted using the near, intermediate and far source seismic records corresponding to the acceleration response spectra envelope shown in Fig. 3. For a given ground motion record, orthogonal combinations (100% in one direction with 30% in the orthogonal direction) were also included in the analyses. The spine model with fixed-base shafts was used for simplicity. The main purpose of the analyses was to verify that hinging at the base of the shafts does not take place.

The elastic moment demand normalized by the nominal moment capacity of a typical shaft (at support#8) is shown in Fig. 8. As expected, the maximum demand was found to be less than half the capacity for all records (and directions of analysis and orthogonal combinations). For other shafts, the maximum demand-to-capacity ratio was less than 0.6.

In order to quantify the efficiency of the isolators, a hypothetical version of the Portacuelo viaduct with no isolators was also modelled assuming a continuous pin support of the superstructure at every bent location. The moment demand to capacity ratio of a typical shaft was also calculated for all the ground motions under consideration. The results are also shown in Fig. 8, from which it is apparent that nonlinear behaviour of the shafts may be expected. The demand to capacity ratio increases by a factor of three in relation to the base isolated superstructure.

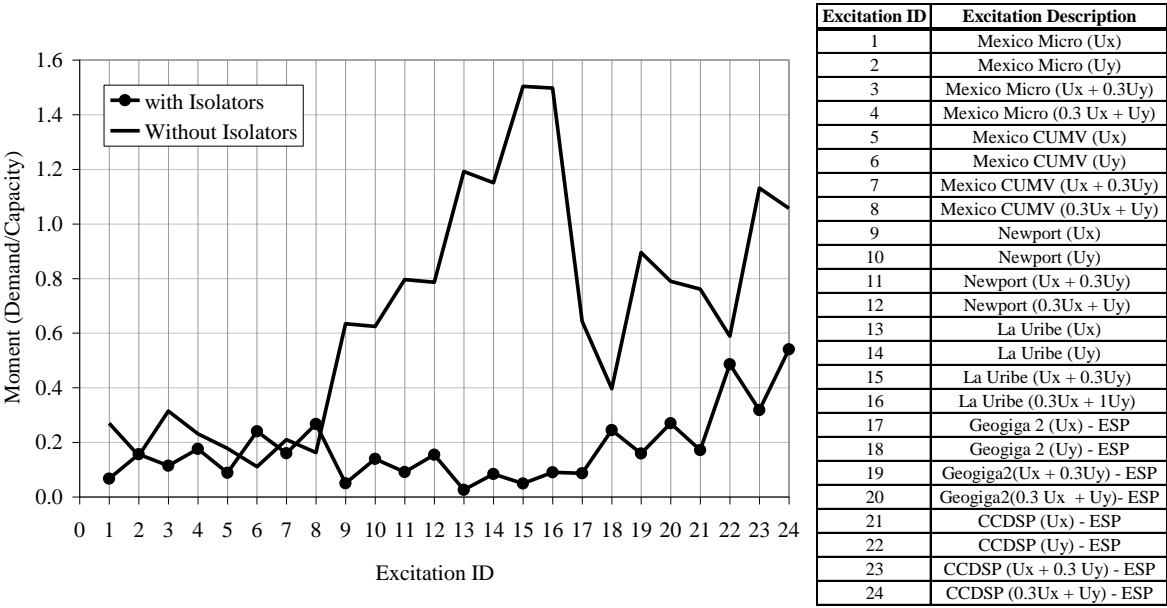


Figure 8. Flexural demand to capacity ratios for a typical shaft of Portachuelo Viaduct with and without isolator

7. CONCLUSIONS

Simplified analysis of the Portachuelo Viaduct as a Single Degree of Freedom (SDOF) system proved to be a valuable tool to characterize the structure and produced results that are consistent with detailed Finite Elements models and measured ambient/traffic vibrations despite the curvature and complex geometrical configuration of the structure. Dynamic linear elastic analyses confirm that for the expected level of ground shaking at the site, forces demands are well-below those that could cause flexural hinging or shear failure. Despite the negligible energy dissipation capacity of the isolators, these still serve the purpose of protecting the substructure from damage under the design ground motions

REFERENCES

- AASHTO Guide Specifications for Seismic Isolation Design (2010), 3rd Edition, American Association of State Highway and Transportation Officials, Washington, D.C., USA
- AASHTO LRFD Bridge Design Specifications (2010), 5th Edition, American Association of State Highway and Transportation Officials, Washington, D.C., USA
- Martínez, Alejandro, Carlos Alvarado, and Diana Rubiano (2002). Selección de señales de diseño consistentes con el escenario regional de amenaza sísmica: Casos aplicados en Colombia. Instituto de Investigación e Información Geocientífica, Minero-Ambiental y Nuclear, INGEOMINAS, Sede Bogotá.
- Matlock, H. (1970). Correlations for design of laterally loaded piles in soft clay. Proceedings, Offshore Technology Conference, **Vol. I**: Paper No. 1204, 577-594, Houston, USA.
- Ministerio de transporte de Colombia (1995). Código Colombiano de Diseño Sísmico de Puentes, Asociación Colombiana de Ingeniería Sísmica.
- Reese, L. C., Cox, W. R., and Koop, F. D. (1974). Analysis of laterally loaded piles in sand. *Proc. Offshore Technology Conference*, **Vol. II**: Paper 2080, 473-484, Houston, USA.
- Stanton, J.F., Roeder C. W., Mackenzie-Helnwein, P., White, C. Cuester, C., Craig, B (2008). Rotation Limits for Elastomeric Bearings. NCHRP Report No. 596, Transportation Research Board, Washington D.C, USA.
- Ventura, C.E., W.D. Liam Finn, J.-F. Lord, and N. Fujita (2003). Dynamic characteristics of a base isolated building from ambient vibration measurements and low level earthquake shaking. *Soil Dynamics and Earthquake Engineering*, **23:4**, 313-322.
- Vucetic, M. and Dobry, R. (1991). Effect Of Soil Plasticity on Cyclic Response, *ASCE Journal of Geotechnical Engineering*, **117:1**, 89-107